







Impact of Turbulent-Flow-Induced Scintillation on Deep-Ocean Wireless Optical Communication

Yang Weng , *Student Member, IEEE*, Yujian Guo , *Student Member, IEEE*, Omar Alkhazragi , *Student Member, IEEE*, Tien Khee Ng , *Senior Member, IEEE, Senior Member, OSA*, Jen-Hwa Guo , *Member, IEEE*, and Boon S. Ooi , *Senior Member, IEEE, Fellow, OSA*

Abstract—The use of autonomous underwater vehicles (AUVs) is highly desirable for collecting data from seafloor sensor platforms within a close range. With the recent innovations in underwater wireless optical communication (UWOC) for deep-sea exploration, UWOC could be used in conjunction with AUVs for high-speed data uploads near the surface. In addition to absorption and scattering effects, UWOC undergoes scintillation induced by temperature- and salinity-related turbulence. However, studies on scintillation have been limited to emulating channels with uniform temperature and salinity gradients, rather than incorporating the effects of turbulent motion. Such turbulent flow results in an ocean mixing process that degrades optical communication. This study presents a turbulent model for investigating the impact of vehicle-motion-induced turbulence via the turbulent kinetic energy dissipation rate. This scintillation-related parameter offers a representation of the change in the refractive index due to the turbulent flow and ocean mixing. Monte Carlo simulations are carried out to validate the impact of turbulent flow on optical scintillation. In experimental measurements, the scintillation index (SI) and signal-to-noise ratio (SNR) are similar with (SI = 0.4824; SNR = 5.56) and without (SI = 0.4823; SNR = 5.87) water mixing under uniform temperature channels. By introducing a temperature gradient of 4 °C, SI (SNR) with and without turbulent flow changed to 0.5417 (5.06) and 0.8790 (3.40), respectively. The experimental results show a similar trend to the simulation results. Thus, turbulent flow was shown to significantly impact underwater optical communications.

Index Terms—Autonomous underwater vehicles, ocean mixing, scintillation, underwater optical communication.

I. INTRODUCTION

UNDERSEA exploration is highly attractive for both general research and military applications. Conventionally,

Manuscript received November 12, 2018; revised April 19, 2019; accepted July 7, 2019. Date of publication July 15, 2019; date of current version September 24, 2019. This work was supported in part by the King Abdullah University of Science and Technology (KAUST) baseline funding under Grant BAS/1/1614-01-01, in part by KAUST equipment funding under Grant KCR/1/2081-01-01 and Grant GEN/1/6607-01-01, and in part by KAUST-KFUPM Special Initiative (KKI) Program under Grant REP/1/2878-01-01. (*Corresponding author: Boon S. Ooi.*)

Y. Weng and J.-H. Guo are with the Department of Engineering Science and Ocean, Engineering National Taiwan University, Taipei 106, Taiwan (e-mail: r04525095@ntu.edu.tw; jguo@ntu.edu.tw).

Y. Guo, O. Alkhazragi, T. K. Ng, and B. S. Ooi are with the Computer, Electrical and Mathematical Sciences and Engineering Division, King Abdullah University of Science and Technology, Thuwal 23955-6900, Saudi Arabia (e-mail: yujian.guo.1@kaust.edu.sa; omar.alkhazragi@kaust.edu.sa; tienkhee.ng@kaust.edu.sa; boon.ooi@kaust.edu.sa).

Color versions of one or more of the figures in this paper are available online at <http://ieeexplore.ieee.org>.

Digital Object Identifier 10.1109/JLT.2019.2928465

research communities deploy observatories on the seafloor to collect *in situ* environmental data and retrieve the data for analysis. Gathering observation data is particularly challenging as physically retrieving the sensor platforms for data upload is time-consuming and expensive [1]–[3]. Wirelessly retrieving sensor data is rarely achieved due to limited bandwidth and interference of the acoustic channel. To this end, the data mule method, shown in Fig. 1, utilizes autonomous underwater vehicles (AUVs) to collect data from seafloor platforms using a close-range wireless optical link before returning to surface for data upload. Optical communication technology is advantageous because of its wide bandwidth and high data rate. Since 2015, which was the early stage of underwater wireless optical communication (UWOC) research, Hassan *et al.* [4] have achieved a 5-m UWOC system with a data rate of 4.8 Gigabits per second (Gbps). In 2017, 20-m UWOC link with 1.5 Gbps data rate was built by Shen *et al.* [5], and Xu *et al.* [6] pushed the data rate to 9.51 Gbps over 10 m. In 2018, a 25-Gbps UWOC system over a 5-m underwater channel was achieved by Li *et al.* [7]. Based on these results, UWOC techniques are expected to be combined with underwater vehicles to improve marine observation in the future [8].

Considering optical beams undergo absorption, scattering, and scintillation in seawater, several channel models have been proposed for characterizing the performance of underwater optical links. Jaruwatanadilok describes the attenuation of optical links in the channel model for absorption and scattering using radiative transfer theory (RTE) [9]. Gabriel *et al.* solved the RTE equations using Monte Carlo simulation and quantified the link performance with different water types and link distances [10]. Najafi *et al.* proposed a model based on the geometric loss to simulate the misalignment issue of FSO channel in drone-based networks [11], which may offer insights for UWOC. Furthermore, the spatial power spectrum of the refractive index (RI) is controlled by temperature and salinity in the ocean medium. Variation in the RI causes the optical intensity to fluctuate randomly, leading to scintillation of the beam, which adversely affects the wireless optical communication quality. Hou utilized an optical turbulence strength parameter that relates to the dissipation rate of temperature or salinity variances to express the RI fluctuation [12]. Jamali *et al.* [13] and Oubei *et al.* [14]–[16] have studied the underwater turbulence introduced by air bubbles, temperature, and salinity. In their research, different probability density functions (PDFs) are used to describe the statistical distribution of different types of turbulence, and the statistical

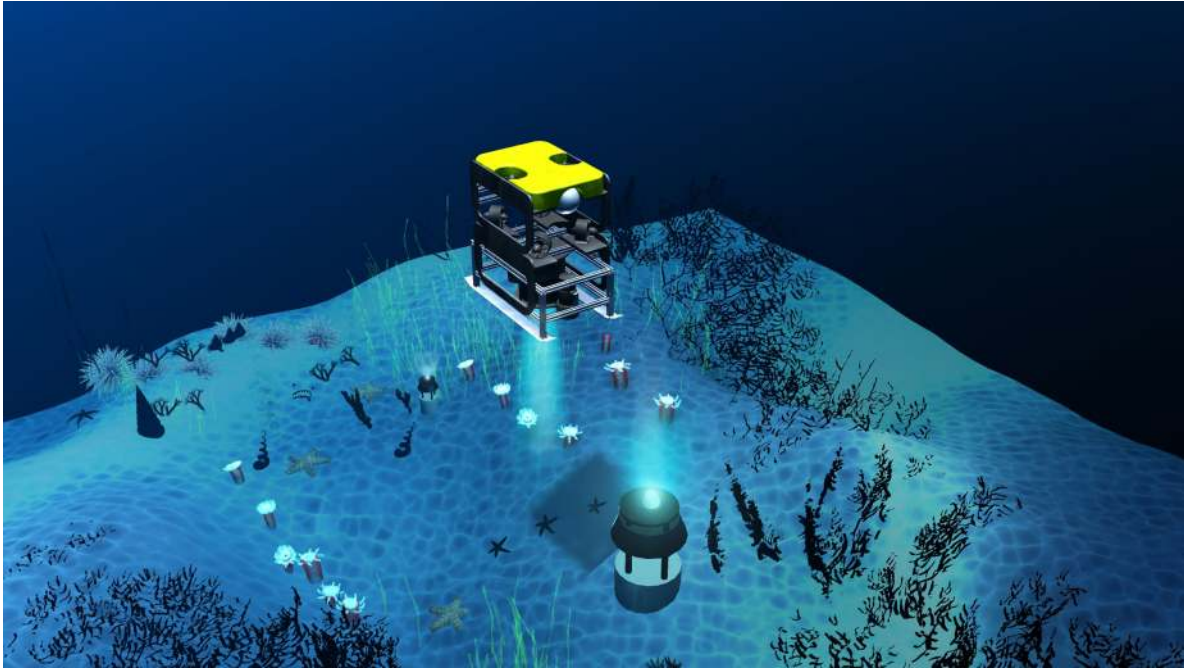


Fig. 1. An autonomous underwater vehicle can serve as a data mule to collect data from seafloor platforms by UWOC. The yellow vehicle designed by National Taiwan University is equipped with six propellers. Turbulent flows will be introduced when the vehicle remains stationary over the observatory during data transmission.

scintillation data was measured. Recent models focus on the relationship between the RI and the thermohaline distribution [17], [18]. Thermohaline diffusivities have an impact on the dissipation rate, and most importantly, these diffusivities are not constant in the presence of turbulence. Thus, the turbulence induced by underwater vehicle motion has a dynamic contribution to the thermohaline dissipation rate. The state of turbulent flow may be a potential determinant for scintillation.

This study is concerned with the influence of propeller-induced turbulent flow on optical beam scintillation based on ocean mixing theory and optical experiments. The propellers mounted in a vehicle can produce velocity shear and increase the turbulence kinetic energy (TKE) dissipation rate, which indicates the turbulence intensity. This turbulence provides energy and drives microscale thermohaline mixing in seawater. Theoretically, the diffusivities of temperature and salinity are positively correlated with the TKE dissipation rate in the mixing process [19]. This research suggests that channel characterization in deep water is profoundly influenced by the emergence of underwater vehicle motion, accompanied by an increase in the TKE dissipation rate and ocean mixing. Meticulous simulation work and experimental study on communication performance of optical systems under different turbulence support this conclusion. Thus, turbulent flow induced by AUV affects optical links. The results of this investigation will expand the applications of underwater vehicles and UWOC in deep-sea exploration.

The remainder of this paper is organized as follows. Section II presents the mechanism of optical scintillation and the function of the TKE dissipation rate. Monte Carlo based simulation results are also presented. Detailed experimental studies are given in Section III. Conclusions are given in Section IV.

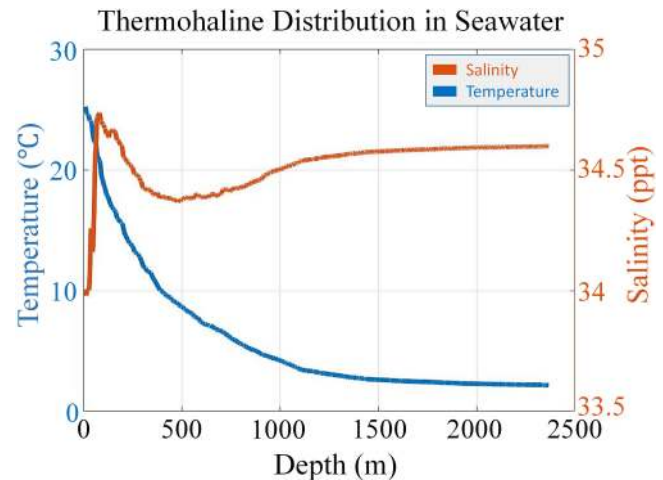


Fig. 2. The temperature and salinity of seawater at 118.6665°E, 20.1683°N (South China Sea) [20].

II. MODEL OF TURBULENCE-INDUCED SCINTILLATION

A. Optical Scintillation

The underwater communication links experience intensity fluctuation when the optical wave propagates through the seawater medium due to the change in the RI along the propagation path. The inhomogeneous RI distribution can be caused by the inhomogeneous thermohaline distribution in seawater. The change in thermohaline characteristics at different depths has been shown in the ocean profile data provided by the world ocean database [20] in Fig. 2. In deep water (>500 m deep), the

gradients of temperature and salinity were $<4^\circ\text{C}$ per kilometer and ~ 0.2 part-per-thousand (ppt) per kilometer, respectively. Quantifying the intensity fluctuations in the thermohaline environment is required before optical channel characterization. The scintillation index (SI) is defined to quantify the optical beam intensity fluctuation and is given by [21]:

$$\sigma^2 = \frac{\overline{I^2} - \bar{I}^2}{\bar{I}^2}, \quad (1)$$

where I is the received intensity of the optical waves, \bar{I} means the mean of I . Following the classical Kolmogorov model for a fully developed turbulent flow, the power spectral density of the RI in seawater is [22]:

$$\Phi_n(\kappa) = 0.388 \times 10^{-8} \phi \varepsilon^{-\frac{1}{3}} \kappa^{-\frac{11}{3}} \left[1 + 2.35(\kappa\eta)^{\frac{2}{3}} \right], \quad (2)$$

with

$$\phi = \frac{\chi_T}{\omega^2} (\omega^2 e^{-A_T \delta} + e^{-A_S \delta} - 2\omega e^{-A_{TS} \delta}), \quad (3)$$

and

$$\delta = 8.284(\kappa\eta)^{\frac{4}{3}} + 12.978(\kappa\eta)^2, \quad (4)$$

where κ is the wavenumber of turbulence and η is Kolmogorov scale. TKE dissipation rate is denoted by ε , the dissipation rate of temperature is represented by χ_T , $A_T = 1.863 \times 10^{-2}$, $A_S = 1.9 \times 10^{-4}$, and $A_{TS} = 9.41 \times 10^{-3}$. The parameter ω , whose values range from -5 to 0 , determines the relative strength of the temperature and salinity in driving the index fluctuations. When salinity-driven turbulence dominates, $\omega = 0$; when temperature-driven turbulence dominates, $\omega = -5$ [23], [24]. The RI model can be simplified in weak fluctuation regimes ($\sigma^2 < 1$), where scintillation index is proportional to Rytov variance [25]:

$$\sigma_R^2 = 37.3 \chi \varepsilon^{-\frac{1}{3}} \left(\frac{2\pi}{\lambda} \right)^{\frac{7}{6}} L^{\frac{11}{6}}, \quad (5)$$

where λ is optical wavelength and L is the migration length of the light beam. χ relates to the dissipation rate of temperature or salinity. As long as there is a gradient or turbulent flow, heat and salts fluxes will exist and continually vary the distributions. Given that the diffusion is homogeneous, the dissipation rates can be defined as:

$$\chi_T = 6k_T \overline{\left(\frac{\partial T'}{\partial z} \right)^2}, \quad (6)$$

$$\chi_S = 6k_S \overline{\left(\frac{\partial S'}{\partial z} \right)^2}, \quad (7)$$

where k_T and k_S are the diffusivity of temperature and salinity, respectively. The fluctuation components, T' and S' , are derived from temperature $T = \bar{T} + T'$, and salinity $S = \bar{S} + S'$, respectively.

Temperature and salinity changes are crucial for Rytov variance. Theoretically, both factors in dissipation rate, diffusivity and gradient are influential for SI. Previous works have investigated the relationship between SI and the gradient in thermohaline distribution [15], [26]. These researches demonstrate that gradients can increase intensity scintillation while diffusivities

are considered as constants. However, the impact of diffusivity on underwater communication link, especially in the presence of motion-induced turbulent flow, is untouched in previous models.

B. Diffusivity in Turbulence-Driven Mixing

Turbulence is described as a very chaotic state of fluid commonly observed in both atmosphere and ocean [27], [28]. A critical feature of the turbulence related to this research is diffusivity, whose coefficient is analogous to, but markedly larger than, molecular diffusivity. The diffusivity is deeply influenced by the ocean mixing process [19]. Turbulence-induced mixing, which is dominant in the ocean, is driven by internal waves and tides, wind stirring, and other shear flows [29]. The propellers mounted in AUVs can introduce the turbulent flow in deep ocean. In the context of fluid dynamics, Navier–Stokes equations can be used to describe the motion of turbulent flows by velocity vector \mathbf{u} , pressure P , viscosity ν , and density ρ [30]:

$$\frac{\partial \mathbf{u}}{\partial t} + \mathbf{u} \cdot \nabla \mathbf{u} = -\frac{\nabla P}{\rho} + \nu \nabla^2 \mathbf{u}. \quad (8)$$

The temperature, salinity, and density, which are considered to be scalars of the fluid, diffuse along with turbulent flows [31]. The second term on the right-hand side of Navier–Stokes equations is a diffusion term. All the scalars of fluid diffuse along the corresponding direction ($i = 1, 2, 3$) can be expressed as:

$$-\overline{u'_i T'} = k_T \frac{\partial T}{\partial z}, \quad (9)$$

$$-\overline{u'_i S'} = k_S \frac{\partial S}{\partial z}, \quad (10)$$

Similar to temperature and salinity, u' is the fluctuation component of velocity. These diffusivities are determined by the turbulent flow state, which supports the conclusion that turbulence affects the thermohaline distribution.

As the equations indicate, the diffusivities of temperature and salinity are in association with the velocity produced by vehicle propellers. To further discuss their relationship, TKE dissipation rate are used to characterize the intensity of this vehicle motion:

$$\varepsilon = \frac{15}{2} \nu \overline{\left(\frac{\partial u'_i}{\partial x} \right)^2}. \quad (11)$$

The expression, which proposed by Osborn, for density diffusivity with regard to TKE dissipation rate can be applied for the thermohaline diffusivities [32]:

$$k_\rho = \frac{R_f \varepsilon}{(1 - R_f) N^2} = \frac{\Gamma \varepsilon}{N^2}, \quad (12)$$

where the Richardson number R_f is defined by the ratio of the buoyancy flux to the turbulent production. Here, N presents the buoyancy frequency. Mixing efficiency Γ is equal to $R_f / (1 - R_f)$, and the value of R_f is derived from ocean observation [33]. Osborn discussed the possibility of a maximum value above which the turbulence cannot be maintained in steady state. Britter's measurements suggested that the critical value for R_f ranges from 0.18 to 0.2 [34], and Osborn recommended the generally accepted value of 0.2 for the mixing efficiency [32].

Therefore, we have:

$$k_\rho = k_T = k_S \leq 0.2 \frac{\varepsilon}{N^2}. \quad (13)$$

The variation of diffusivity caused by propellers can be transmitted to RI and Rytov variance.

C. Motion-Induced Scintillation Model

The theory of ocean mixing process is introduced to refine the underwater optical channel model in this study. Combining (5), (6) and (13), the temperature-related Rytov variance can be expressed by:

$$\sigma_R^2 = 44.76\varepsilon^{\frac{2}{3}} \left(\frac{\partial T'}{\partial z} \right)^2 \left(\frac{2\pi}{\lambda} \right)^{\frac{7}{6}} L^{\frac{11}{6}} N^{-2}. \quad (14)$$

In addition to temperature or salinity gradients, the state of turbulent flows is another determinant for Rytov variance. The TKE dissipation rate becomes an essential parameter regarding scintillation.

It is worth discussing the role of the TKE dissipation rate in the scintillation. Equations (2) and (5) are inversely proportional to the TKE dissipation rate. However, the wrong conclusion [24] may be drawn by assuming that the TKE dissipation rate can decrease the SI. In other words, an increase in TKE dissipation will be incorrectly assumed to have an inverse relation to scintillation without combining with the abovementioned mixing process. The gradients of temperature/salinity is prerequisite. The reason that TKE dissipation is involved in this model is the diffusivity defined in equation (6) and (7). Without the gradient, dissipation rates of temperature and salinity are comparatively low in spite of strong turbulent flows. All these conclusions will be discussed in simulation and experiment results in the following section.

D. Simulation Results

In this paper, we focus on presenting a simple physical simulation model based on Monte Carlo method [35] for a turbulent UWOC horizontal link. The Monte Carlo algorithm is far less computationally intensive compared to the approaches based on computational fluid dynamics. The proposed model is based on the interaction of propagating photons with a turbulent medium, which is presented in consecutive turbulent cells with different RI, denoted as n_i . Each turbulent cell is a unit of seawater medium in which the optical signal propagates. The n_i depends on the temperature of water, T , salinity of water, S , and wavelength of the light, λ . The received intensity of optical signal is calculated based on the fraction of received photons to the transmitted photons. The propagation path of each simulated photon from the transmitter is mainly dependent on the changes of n_i . The photon is assumed to move in a straight line until it reaches the boundary of the following cell. The new direction is then calculated using Snell's law in vector form. The field of view of the receiver is set as 30° and the radius of the receiver's active area is set as 0.1 cm. The channel distance between the transmitter and the receiver is 1 m. The salinity in each cell is equal to 40 ± 0.3 ppt according to the salinity of Red Sea. We

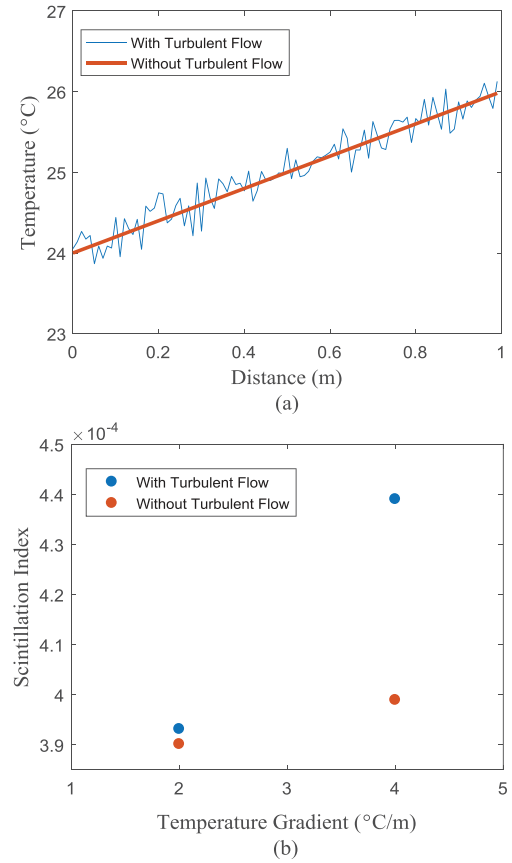


Fig. 3. (a) Temperature profile with and without turbulent flow. (b) Scintillation index at different temperature gradients. The left and right plots are measured without and with mixing, respectively.

characterized the scintillation of links with different temperature gradients.

To create the temperature gradient, we set the temperature on the transmitter's side to the lowest temperature in the gradient with each successive layer having a slightly higher temperature until the maximum value is reached on the receiver's end. However, in the case of turbulent water, the random movement is assumed to move water molecules around, creating random variations in the temperature value. The temperature profiles with and without these random variations with a $2^\circ\text{C}/\text{m}$ gradient are shown in Fig. 3(a). We collected 1,000 intensity samples, for each of which we simulated 10,000 photons, and we calculated the SI values, which are shown in Fig. 3(b). From the SI values, we can see that inducing the random movement in the water increases the severity of the turbulence, resulting in a less stable communication link, this will be verified in the following experiment.

III. EXPERIMENT OF EMULATED TURBULENT FLOW

A. Experimental Setup

Experiments were performed to study the impact of turbulent flows on UWOC quality and the performance of UWOC systems. To simulate the underwater channel, a 1-m long, 0.12-m wide, and 0.12-m high water tank was filled with 6 L of pure

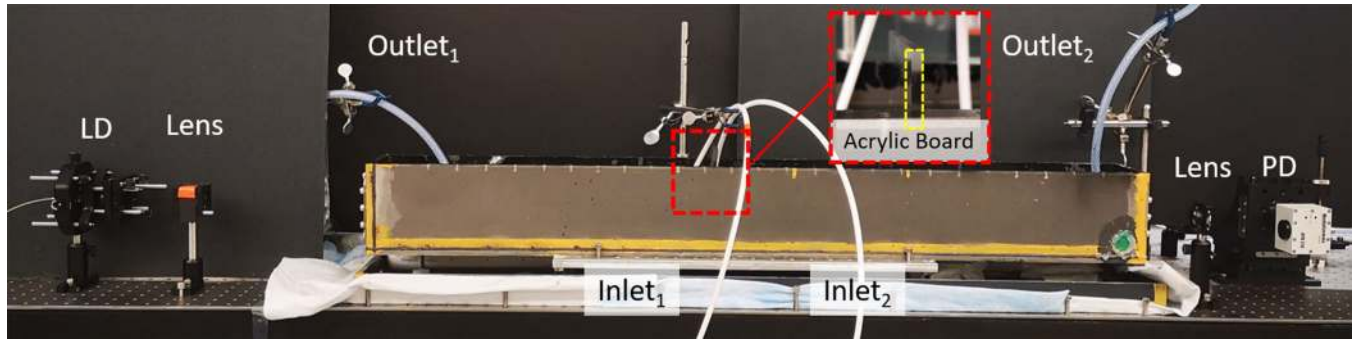


Fig. 4. The experimental setup utilized to study the impact of turbulent flows on wireless optical communication quality. The grey tank is filled with Pure Water Type II, and a laser diode and a photodetector are deployed at opposite ends of the tank.

water (type I) from the water deionizer (Milli-Q Academic, Millipore). The laser diode (LD) and photodetector (PD) were placed on either side of the tank. Two optical windows were mounted in this container for the beam to penetrate. A single mode 520-nm pigtail-fiber LD (LP520-SF15, Thorlabs) served as the transmitter. The beam generated from the green laser was collimated through a plano-convex lens (LA1951-A, Thorlabs), propagated through the tank, and focused again by the same type of lens (LA1951-A, Thorlabs). At the receiver side, the focused beam was detected by the avalanche photodetector (APD 210, Menlo systems). The modulated signal injected to the laser diode was generated by the high-performance serial bit error ratio tester (J-BERT N4903B, Agilent). The bit error ratio (BER) of the communication system was analyzed by this equipment. The eye diagram and histogram analysis were generated by the digital communication analyzer (Infinium DCA-J 86100C, Agilent). The SI was analyzed by the waveform of the received signal collected by the mixed-domain oscilloscope (MDO3104, Tektronix). The experimental setup is shown in Fig. 4.

The optical waves were propagated under three different temperature gradients, and two circulators were used to maintain corresponding gradients. To maintain the water at the desired temperature, the circulator pump was connected to one end of the tank and to a temperature controller (Julabo-F12 chiller). Water at the expected condition was injected into one end of the tank through the circulator. Different temperature conditions at the two circulators produced gradients in the water channel. Obviously, this machine was able to introduce turbulent flows, as the fluid velocity on the wall of the tank was zero. The mixing process altered the temperature distribution, making it more prone to fluctuations. To study the influence of the mixing process, a control group without mixing was employed. The circulators were utilized in the control group for maintaining temperature gradients, and a transparent medium (4-mm-thick acrylic board with a transmission rate up to 92% of visible range) that can transfer heat was placed in the middle of the tank to block the turbulent flow. Under this condition, turbulent flows existed in two zones, but they could only exchange heat through the transparent sheet, which constrained the transfer of fluid scalars. Turbulent flow was introduced in this contrast group to eliminate other potential factors that may affect the optical profile, such as particles in the medium disturbed by flow.

TABLE I
DIFFERENT TEMPERATURE IN CIRCULATOR TO CREATE
TEMPERATURE GRADIENT

Inlet Temperature 1 (°C)	Inlet Temperature 2 (°C)	Temperature Gradient (°C·m ⁻¹)	Mean Temperature (°C)
25	25	0	25
24	26	2	25
23	27	4	25

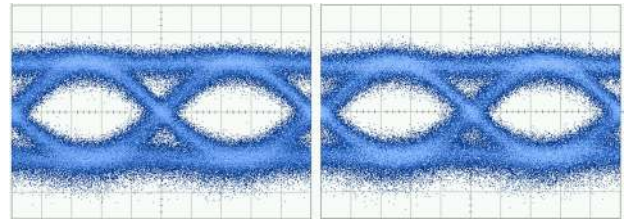


Fig. 5. The eye diagrams of OOK-modulated optical communication in 1-m water tank without the temperature gradient. The left and right plots are derived from measurements without and with turbulent-flow-induced mixing, respectively. Each division represents 32.2 mV.

The two cases of experiments, with and without the mixing process, were performed at three different temperature gradients but same with the simulation conditions, as shown in Table I. The optical signals were modulated by on-off keying (OOK), and the data rate was 1 Gbps. Several parameters, namely the BER, eye diagram, signal-to-noise ratio (SNR), and SI, were measured to characterize the UWOC quality. The SI was calculated on signals without modulation. The influence of turbulent-flow-induced scintillation was determined based on the experimental data.

B. Results and Discussion

The first experiment was conducted under a uniform temperature condition. The eye diagrams of the optical beam without temperature gradient are shown in Fig. 5. The BER of each experimental condition is presented in Table II. The intensity distribution and SI were recorded and presented in Fig. 6 and Table II. Compared to the result of the turbulent flow-induced mixing process, the optical communication qualities without this mixing were almost the same. Thus, the turbulent flow

TABLE II
MEASURED SCINTILLATION INDEX, SIGNAL-TO-NOISE RATIO, AND BIT ERROR RATIO

Experiment Number	1		2		3	
Temperature Gradient	0 °C · m ⁻¹		2 °C · m ⁻¹		4 °C · m ⁻¹	
Mixing Process	No	Yes	No	Yes	No	Yes
Scintillation Index	0.4823	0.4824	0.5092	0.5610	0.5417	0.8790
Minimum SNR	5.86	5.53	5.23	4.13	1.68	1.29
Maximum SNR	5.87	5.56	5.27	4.19	5.06	3.40
BER	0.93×10^{-7}	1.05×10^{-7}	1.21×10^{-6}	3.58×10^{-4}	5.35×10^{-4}	1.42×10^{-1}

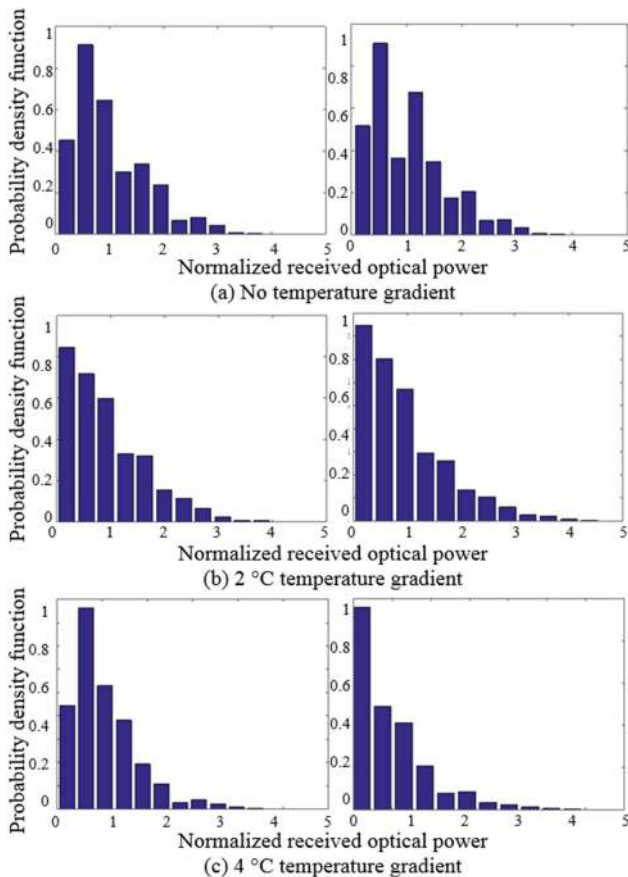


Fig. 6. Normalized received optical intensity distribution (a) without temperature gradient, and at temperature gradients of (b) 2 °C, and (c) 4 °C. The left and right plots are measured without and with mixing, respectively.

seldom disturbs the density distribution. According to (6), the dissipation rate of the temperature is extremely low if there is no temperature gradient. The experimental results show that turbulent flow does not influence the performance of UWOC when the temperature was uniformly distributed. In other words, these controlled groups demonstrate that a temperature gradient is a prerequisite for scintillation. Beam fluctuation is evitable in turbulent flow. A temperature gradient occurs in the second experiment where the inlet water temperatures from the two

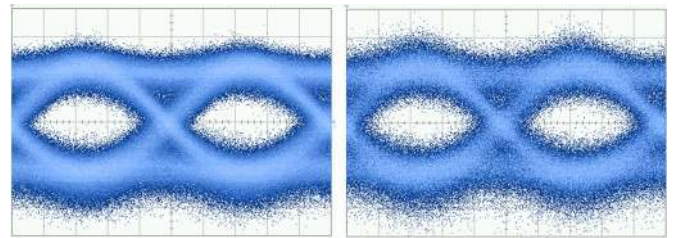


Fig. 7. The eye diagrams of OOK modulated optical communication in the 1-m water tank with 2-°C temperature gradient. The left and right plots are derived from measurements without and with turbulent-flow-induced mixing, respectively. Each division represents 32.2 mV.

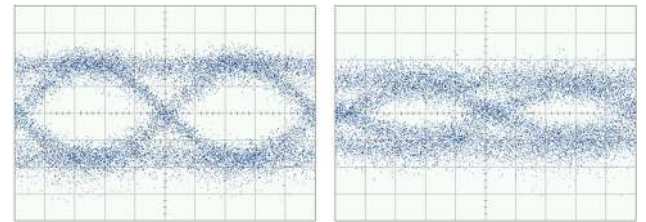


Fig. 8. The eye diagrams of OOK-modulated optical communication in the 1-m water tank with 4-°C temperature gradient. The signal fluctuates between these two patterns due to strong scintillation. Each division represents 32.2 mV. No turbulent flow was induced.

circulators are set to 24 °C and 26 °C. The BER increases compared to that in the first experiment. The introduction of a temperature gradient aggravates beam fluctuation. The measured eye diagrams under this situation are shown in Fig. 7. The values in the no mixing group and mixing group differ by two orders of magnitude, which shows that turbulent-flow-induced mixing contributes to scintillation. This difference is evident in both the eye diagram and the SI (Table II). Thus, turbulent flow can seriously affect the optical pattern in the same gradient medium.

The temperature gradient was expanded to 4 °C per meter in the third experiment. The scintillation was more severe than that in the 2 °C gradient case. The BER increases accordingly. The eye diagram was difficult to record because the signals vibrated frequently. As shown in Fig. 8 and Fig. 9, the amplitude was reduced by at least half of that of 2 °C temperature gradient.

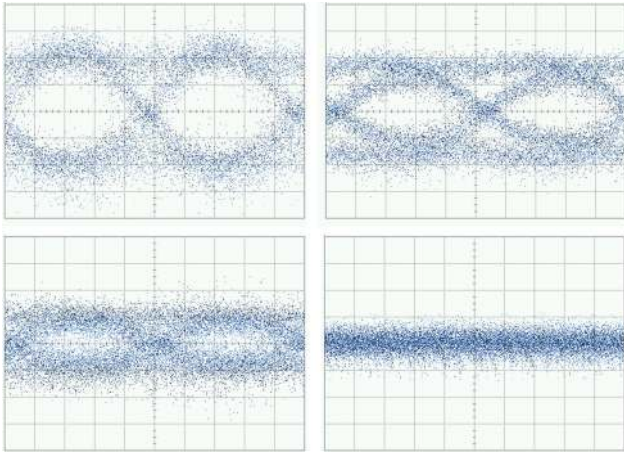


Fig. 9. The eye diagrams of OOK-modulated optical communication in the 1-m water tank with 4-°C temperature gradient. The signal fluctuates between these four patterns due to strong scintillation caused by temperature gradient and turbulent flow. Each division represents 32.2 mV.

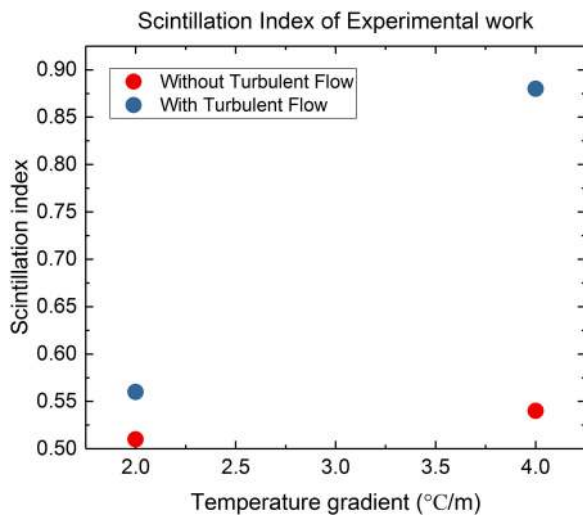


Fig. 10. Scintillation index at different temperature gradients by experimental work. The left and right plots are measured without and with mixing, respectively.

In some cases, the signals in the group with the mixing process may have the same order of amplitude as noise because of the scintillation. The SNR quantifies these results. The minimum and maximum SNR of 4 °C gradient mixing group are 1.29 dB and 3.40 dB, respectively, while the corresponding SNR in 2 °C gradient group are 4.13 dB and 4.19 dB. The BER and SI also reflect the poor communication quality. The recorded BER was 1.42×10^{-1} , which can barely be corrected under current error correction codes. From the measurements, the performance degrades as the temperature gradient increases. If turbulent flow exists, the communication quality degrades further. In fact, the BER under the condition of a 2-°C gradient with mixing was higher than that under a 4-°C gradient without mixing.

The experimental results, shown in Fig. 10, have the same trend with the simulation results. It is important to note that the simulation does not take into account the noise of the electrical part in the system, especially the noise from the APD used in the

experiment. Guo *et al.* mentioned the APD noise affects the SI values in their reciprocal turbulence research in underwater environment [26]. For that reason, the SI values obtained from the simulation are lower. The same trend shown by the simulation and experiment supports the conclusion proposed in Section II that the turbulent-flow-induced mixing process promotes diffusion efficiency, which positively facilitates scintillation.

IV. CONCLUSIONS

This paper investigated the relationship between turbulent-flow-induced mixing process and scintillation in UWOC because communication quality is crucial when underwater vehicles equipped with wireless optical systems are used to collect data from seafloor platforms. We considered the modelling of the influence of turbulent-flow induced mixing process on scintillation of underwater optical links. The Monte Carlo based simulation was applied to verify the model. Furthermore, we validated the model and simulation results via experimental work. From the experiment results, we concluded that turbulent flow should be taken into account in underwater wireless optical channel models because turbulent flow can significantly affect the optical pattern in the gradient medium. For future work, simulation method can focus on the scintillation of received optical intensity, beam misalignment issues, and turbulence induced by the instability of AUV in case of transmitters and receivers are carried by the AUV. Following the simulation, the technique can be tested in field experiment to improve the performance of localization and navigation algorithm for AUV in data mule task. In future work on mitigation strategies, the aperture averaging technique is considered to be a potential technique for combating scintillation. This method avoids receiving waves from a single propagation path, and the averaging of identical apertures erases relatively fast fluctuations due to small turbulence. Significantly, the fading of received signals become smoother after using this technique. Hence, this research expands future applications for underwater vehicles using wireless optical communication in deep-sea exploration.

REFERENCES

- [1] H. Brundage, "Designing a wireless underwater optical communication system," M.S. thesis, Dept. Mech. Eng., Massachusetts Inst. Technol., Cambridge, MA, USA, 2010.
- [2] C. Pontbriand *et al.*, "Wireless data harvesting using the AUV sentry and WHOI optical modem," in *Proc. OCEANS'15 - MTS/IEEE Conf.*, Washington, DC, USA, 2015, pp. 1–6.
- [3] J. Hansen *et al.*, "Autonomous acoustic-aided optical localization for data transfer," in *Proc. OCEANS'15-MTS/IEEE Conf.*, Washington, DC, USA, 2015, pp. 1–7.
- [4] H. M. Oubei *et al.*, "4.8 Gbit/s 16-QAM-OFDM transmission based on compact 450-nm laser for underwater wireless optical communication," *Opt. Express*, vol. 23, no. 18, pp. 23302–23309, 2015.
- [5] C. Shen *et al.*, "20-meter underwater wireless optical communication link with 1.5 Gbps data rate," *Opt. Express*, vol. 24, no. 22, pp. 25502–25509, 2016.
- [6] M. Kong *et al.*, "10-m 9.51-Gb/s RGB laser diodes-based WDM underwater wireless optical communication," *Opt. Express*, vol. 25, no. 17, pp. 20829–20834, 2017.
- [7] C.-Y. Li *et al.*, "A 5 m/25 Gbps underwater wireless optical communication system," *IEEE Photon. J.*, vol. 10, no. 3, Jun. 2018, Art. no. 7904909.

- [8] Y. Weng, J. Guo, A. Hsiao, and S.-W. Huang, "Vehicle motion on optical communication quality in the process of underwater wireless data upload," in *Proc. OCEANS'17*, Anchorage, AK, USA, 2017, pp. 1–5.
- [9] S. Jaruwatanadilok, "Underwater wireless optical communication channel modeling and performance evaluation using vector radiative transfer theory," *IEEE J. Sel. Areas Commun.*, vol. 26, no. 9, pp. 1620–1627, Dec. 2008.
- [10] C. Gabriel, M. A. Khalighi, S. Bourennane, P. Leon, and V. Rigaud, "Monte-Carlo-based channel characterization for underwater optical communication systems," *IEEE J. Opt. Commun. Netw.*, vol. 5, no. 1, pp. 1–12, 2013.
- [11] M. Najafi, H. Ajam, V. Jamali, P. D. Diamantoulakis, G. K. Karagiannidis, and R. Schober, "Statistical modeling of FSO fronthaul channel for drone-based networks," in *Proc. IEEE Int. Conf. Commun.*, 2018, pp. 1–7.
- [12] W. W. Hou, "A simple underwater imaging model," *Opt. Lett.*, vol. 34, no. 17, pp. 2688–2690, 2009.
- [13] M. V. Jamali *et al.*, "Statistical studies of fading in underwater wireless optical channels in the presence of air bubble, temperature, and salinity random variations," *IEEE Trans. Commun.*, vol. 66, no. 10, pp. 4706–4723, Oct. 2018.
- [14] H. M. Oubei, R. T. ElAfandy, K.-H. Park, T. K. Ng, M.-S. Alouini, and B. S. Ooi, "Performance evaluation of underwater wireless optical communications links in the presence of different air bubble populations," *IEEE Photon. J.*, vol. 9, no. 2, pp. 1–9, Mar. 2017.
- [15] H. M. Oubei *et al.*, "Simple statistical channel model for weak temperature-induced turbulence in underwater wireless optical communication systems," *Opt. Lett.*, vol. 42, no. 13, pp. 2455–2458, Jul. 2017.
- [16] H. Makine Oubei *et al.*, "Efficient Weibull channel model for salinity induced turbulent underwater wireless optical communications," in *Proc. 12th Conf. Lasers Electro-Opt. Pac. Rim*, Singapore, 2017, pp. 1–2.
- [17] M. Yousefi, S. Golmohammady, A. Mashal, and F. D. Kashani, "Analyzing the propagation behavior of scintillation index and bit error rate of a partially coherent flat-topped laser beam in oceanic turbulence," *J. Opt. Soc. Amer. A*, vol. 32, no. 11, pp. 1982–1992, Nov. 2015.
- [18] X. Yi, Z. Li, and Z. Liu, "Underwater optical communication performance for laser beam propagation through weak oceanic turbulence," *Appl. Opt.*, vol. 54, no. 6, pp. 1273–1278, Feb. 2015.
- [19] R. W. Schmitt, J. Ledwell, E. Montgomery, K. Polzin, and J. Toole, "Enhanced diapycnal mixing by salt fingers in the thermocline of the tropical Atlantic," *Science*, vol. 308, no. 5722, pp. 685–688, Apr. 2005.
- [20] T. P. Boyer *et al.*, World Ocean Database, 2013. [Online]. Available: https://www.nodc.noaa.gov/OC5/WOD/pr_wod.html
- [21] L. C. Andrews, R. L. Phillips, C. Y. Hopen, and M. Al-Habash, "Theory of optical scintillation," *J. Opt. Soc. Amer. A*, vol. 16, no. 6, pp. 1417–1429, Jun. 1999.
- [22] V. Nikishov and V. Nikishov, "Spectrum of turbulent fluctuations of the sea-water refraction index," *Int. J. Fluid Mech. Res.*, vol. 27, no. 1, pp. 82–98, 2000.
- [23] W. Lu, L. Liu, and J. Sun, "Influence of temperature and salinity fluctuations on propagation behaviour of partially coherent beams in oceanic turbulence," *J. Opt. A*, vol. 8, no. 12, pp. 1052–1058, Nov. 2006.
- [24] Y. Ata and Y. Baykal, "Scintillations of optical plane and spherical waves in underwater turbulence," *J. Opt. Soc. Amer. A*, vol. 31, no. 7, pp. 1552–1556, Nov. 2014.
- [25] W. Liu, Z. Xu, and L. Yang, "SIMO detection schemes for underwater optical wireless communication under turbulence," *Photon. Res.*, vol. 3, no. 3, pp. 48–53, Jun. 2015.
- [26] Y. Guo *et al.*, "On the reciprocity of underwater turbulent channels," *IEEE Photon. J.*, vol. 11, no. 2, pp. 1–9, Apr. 2019, Art. no. 7901909.
- [27] H. L. Grant, R. W. Stewart, and A. Moilliet, "Turbulence spectra from a tidal channel," *J. Fluid Mech.*, vol. 12, no. 2, pp. 241–268, Feb. 1962.
- [28] G. I. Taylor, "The spectrum of turbulence," *Proc. Roy. Soc. A*, vol. 164, no. 919, pp. 476–490, Feb. 1938.
- [29] A. Wüest, G. Piepke, and D. C. Van Senden, "Turbulent kinetic energy balance as a tool for estimating vertical diffusivity in wind-forced stratified waters," *Limnol. Oceanogr.*, vol. 45, no. 6, pp. 1388–1400, Sep. 2000.
- [30] A. J. Chorin, "Numerical solution of the Navier-Stokes equations," *Math Comput.*, vol. 22, no. 104, pp. 745–762, 1968.
- [31] V. M. Canuto, A. Howard, Y. Cheng, and M. Dubovikov, "Ocean turbulence. Part I: One-point closure model—Momentum and heat vertical diffusivities," *J. Phys. Oceanogr.*, vol. 31, no. 6, pp. 1413–1426, Jun. 2001.
- [32] T. Osborn, "Estimates of the local rate of vertical diffusion from dissipation measurements," *J. Phys. Oceanogr.*, vol. 10, no. 1, pp. 83–89, Jan. 1980.
- [33] L. St. Laurent and R. W. Schmitt, "The contribution of salt fingers to vertical mixing in the north Atlantic tracer release experiment," *J. Phys. Oceanogr.*, vol. 29, no. 7, pp. 1404–1424, Jul. 1999.
- [34] R. Britter, "An experiment on turbulence in a density stratified fluid," Ph.D. dissertation, Monash Univ., Clayton, VIC, Australia, 1974.
- [35] Z. Vali, A. Gholami, Z. Ghassemloooy, D. G. Michelson, M. Omoomi, and H. Noori, "Modeling turbulence in underwater wireless optical communications based on Monte Carlo simulation," *J. Opt. Soc. Amer. A*, vol. 34, no. 7, pp. 1187–1193, 2017.

Yang Weng (S'15) received the B.S. degree in telecommunication engineering from Ocean University of China, Qingdao, China, in 2015, and the M.S. degree in engineering science and ocean engineering from National Taiwan University, Taipei, Taiwan, China, in 2018. From 2018 to 2019, he was a Visiting Student with the Photonics Laboratory, King Abdullah University of Science and Technology (KAUST), Thuwal, Saudi Arabia. His research interests include underwater wireless optical communication and the navigation of autonomous underwater vehicles.

Yujian Guo (S'18) received the Bachelor's degree in electrical engineering from the University of Electronic Science and Technology of China, Chengdu, Sichuan, China, in 2017. He is currently working toward the Ph.D. degree in the Department of Computer, Electrical and Mathematical Sciences & Engineering, King Abdullah University of Science and Technology (KAUST), Saudi Arabia. His current research interests include underwater wireless optical communications and underwater optical channel characterization.

Omar Alkhazragi (S'19) received the Bachelor of Science in Electrical Engineering degree in 2018 from the King Fahd University of Petroleum and Minerals (KFUPM), Saudi Arabia. He is currently working toward the M.S./Ph.D. degree in electrophysics in the Photonics Laboratory, King Abdullah University of Science and Technology (KAUST), Saudi Arabia. The primary focus of his research is on studying optical wireless communication systems experimentally and theoretically.

Tien Khee Ng (SM'17) received the M.Eng. and Ph.D. degrees in electrical and electronic engineering from Nanyang Technological University, Singapore, in 2001 and 2005, respectively. He is currently a Senior Research Scientist with Ooi-Group, King Abdullah University of Science and Technology (KAUST), Saudi Arabia, and the Co-Principal-Investigator responsible for the molecular beam epitaxy thrust for the KACST Technology Innovation Center for Solid-State Lighting at KAUST. His research primarily focuses on the development of wide bandgap nitride quantum-confined and nanowires structures for addressing efficient light emitters, optical communications, and energy harvesting. He is a Member of SPIE and a Senior Member of the Optical Society (OSA).

Jen-Hwa Guo (M'92) received the Ph.D. degree in mechanical engineering from the University of Minnesota, Twin Cities, MN, USA, in 1992. He is currently a Professor with the Department of Engineering Science and Ocean Engineering, National Taiwan University, Taipei, Taiwan. He was the Head of the Marine Exploration Technology Division, Taiwan Ocean Research Institute for the Deep-Sea Scientific ROV Research and Development project, from 2008 to 2012, and has been involved in several unmanned underwater vehicle development projects. His current research interests include the sensing and control of biomimetic underwater robots, the navigation of autonomous surface vehicle fleets, and AUV applications in the underwater archaeology.

Boon S. Ooi received the Ph.D. degree from the University of Glasgow, Glasgow, U.K., in 1994. He joined the King Abdullah University of Science and Technology (KAUST) from Lehigh University (USA) in 2009. He is currently a Professor of electrical engineering with KAUST. His recent research work is concerned with the study of III-nitride based materials and devices, lasers for applications, such as solid-state lighting, visible light, and underwater wireless optical communications, and energy-harvesting devices. He has served on the technical program committee of CLEO, IPC, ISLC, and IEDM. He currently serves on the editorial board of *Optics Express* and *IEEE PHOTONICS JOURNAL*. He is a Fellow of OSA, SPIE, and IoP (U.K.).